RARE METALS
Vol. 28, Spec. Issue, Oct 2009, p. 46

Semiconductor nanostructure growth and device application

WANG Z. G., LIU F. Q., CHEN Y. H., XU B., JIN P., and WU J.

Key Lab of Semiconductor Materials Science, Institute of Semiconductors, Chinese Academy of Sciences, Beijing 100083, China

Received 5 July 2009; received in revised form 1 August 2009; accepted 10 August 2009

Abstract: Most new concept quantum devices are based on semiconductor nanostructures. Quantum dots (QDs) and quantum wells (QWs) are basic units of semiconductor nanostructures. Here we report issues related to molecular-beam epitaxial (MBE) growth of QD and QW structures. The evolution of InAs/(In)GaAs wetting layer (WL) and QD is disclosed by using reflectance difference spectroscopy (RDS) and atomic force microscopy (AFM) technique. Controlled growth of high performance of quantum dot lasers and quantum dot super luminescent diodes are achieved. By proper using the strain technique, strain-compensated $In_xGa_{1-x}As/In_yAl_{1-y}As$ quantum cascade laser (QCL) materials are grown. Room temperature continuous wave operation of QCLs with $\lambda \approx 7.4$ and 4.6 μm are presented.

The fabrication of quantum dots (QDs) and quantum wells (QWs) have been intensively investigated in the last decade for basic physics and device applications. However, in spite of the development of various growth methods, many hurdles still remain which have to be overcome for the realization of QD and QW devices with the predicted properties.

QDs formed in the Stranski-Krastanow growth mode are not well controlled in dot size and shape, special distribution, exact dot density, modulated doping etc. To improve the optical quality of QDs, some issue related to the strain, coupling and wetting layers (WLs) should be disclosed. The investigation on the behavior of InAs wetting layer (WL) during the molecular-beam epitaxial (MBE) growth of InAs quantum dots (QDs) is very important in both fundamental research and practical application. It is commonly accepted that the WL takes a significant part in the self-assembling of InAs QDs, as well as in the dynamics of electrons in a working device based on QDs. However, the evolution of the InAs WL with increasing InAs deposition θ during the epitaxial growth of InAs on GaAs(001) is far from being clarified at present time. Here, the behavior of the InAs WL with increasing θ was investigated by both reflectance difference spectroscopy (RDS) and atomic force microscopy (AFM). Typical results are shown in Fig. 1. Two peaks were identified in the RDS as related to the heavy- and light-hole states, respectively, in the wetting layer. From the intensity and the position of the two RDS peaks, the segregation behavior happening in the InAs WL and the variation in the in-plane optical anisotropy (OA) with increasing θ are observed. The critical behavior in the two-/three-dimensional (2D/3D) growth mode transition was also observed in RDS. It was found that the critical thickness θ_c of the 2D/3D transition as determined in RDS measurement is quite different from that as determined by AFM when the growth temperature is higher than 510 ℃.

Furthermore, a detailed observation was made using AFM on the 2D/3D transition in the InAs/GaAs(001) system. It was found that the evolution of the InAs quantum dots in the 2D/3D transition depends on the depositing mode during MBE. In the conventional MBE, the evolution of InAs QDs can be divided into two successive regimes according to the distinctive size distributions and different power laws for the variation of the QDs area density N with increasing θ, $N \sim (\theta - \theta_C)^{-\alpha_i}$ (Fig. 2). In the first regime with $\alpha_i = 1.8$, the QDs height distribution is a monotonically decreasing function. The first regime may be explained in terms of a critical phenomenon in a continuous phase transformation. Fort the second regime with $\alpha_i = 0.3$, the QD height distribution can be approximated as a Gaussian type. However, in the case of migration enhanced epitaxy (MEE), the area density *N increases linearly with* θ in a relatively large range of θ, with the height distribution similar to that of the MBE QDs. The difference in the evolution of InAs QDs between the conventional MBE and the MEE was verified.

Corresponding author: WANG Z. G. **E-mail**: zgwang@semi.ac.cn

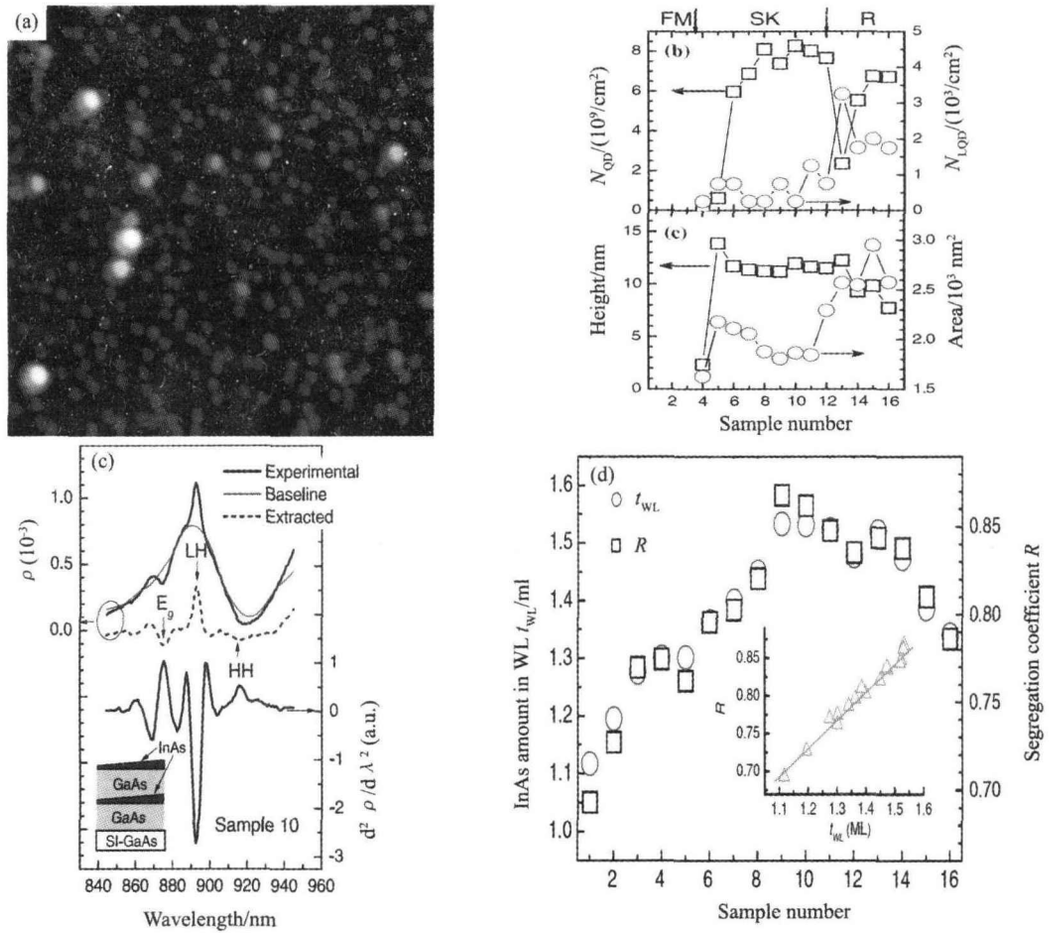

Fig. 1. Typical AFM image of InAs QDs (a), statistics of AFM results (b), corresponding RDS result (c), segregation coefficient R versus InAs amount in WL (d).

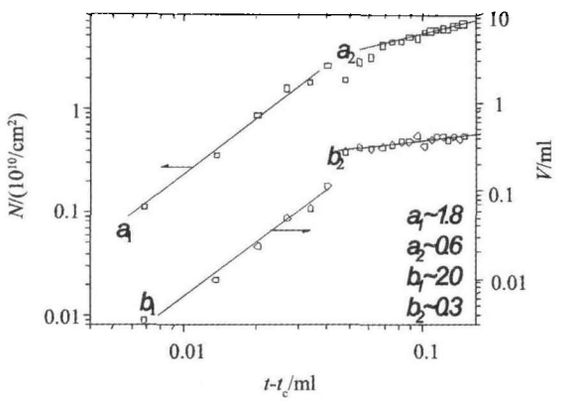

Fig. 2. The evolution of QDs in a small InAs deposition range obeys power law of $N \sim (\theta - \theta_c)^{\alpha_i}$, and can be divided into two regimes.

The above result provides a reference on improving the quality of QDs nanostructures. After adjusting the growth parameters like initializing In(Ga)As nominal composition, specific flux ratios, growth temperature and growth rate for different layers, we have grown high power and long lifetime QD Laser (Fig. 3), InP based 1.73 μm InAs quantum wires (QWRs) laser (Fig. 4), and room temperature CW operated high power QD super luminescent diodes (SLD) (Fig. 5).

For InP-based QCLs, the strain-compensated $In_xGa_{(1-x)}As/In_yAl_{(1-y)}As$ was employed as the active regions, which were specifically designed for emission at 7.4 and 4.6 μm, respectively, using a double-phonon resonant method. Our MBE system is a solid source MBE equipped with valved crackers for the phosphorus and arsenic sources. Laser wafers with active region of 30-35 periods were grown on n-doped ($2\text{-}4\times10^{17}$ cm^{-3}) InP substrates. 2-2.5 μm-thick n-InP layers with graded doping (6×10^{16}-5×10^{18} cm^{-3}) are used as upper cladding layers. The strain-compensated $In_xGa_{(1-x)}As/In_yAl_{(1-y)}As$ structures were grown at a substrate temperature of 505 ℃. Typical MBE growth rates, 0.62-0.95 μm/h for strained $In_xGa_{(1-x)}As$ and 0.75-1.3 μm/h for strained $In_yAl_{(1-y)}As$ were used during wafers growth. The thick InP layers were grown at a substrate temperature of 490 ℃ and growth rate of 0.75 μm/h.

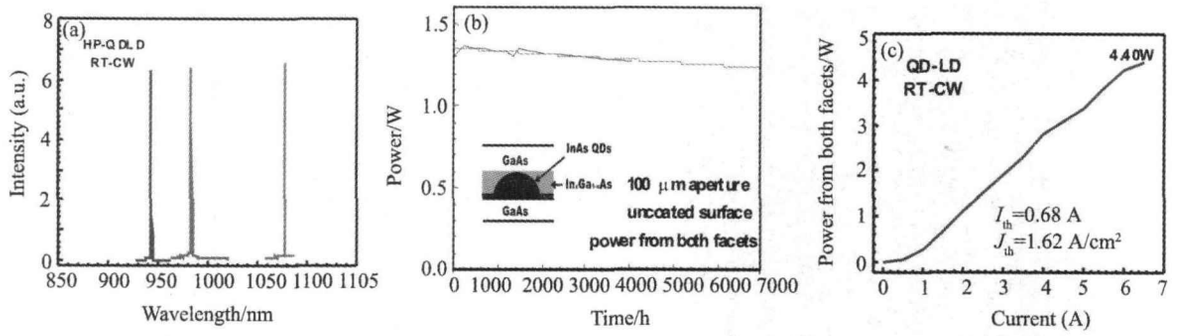

Fig. 3. RT CW operation with λ from 940 to 1160 nm, (b) QD laser lifetime (*RT* 1.3 W CW operation) is more than 7000 h at -0.5 db, (c) typical I-V curve of a QD laser, J_{th}≈160 A/cm², P_{max}=4.4 W.

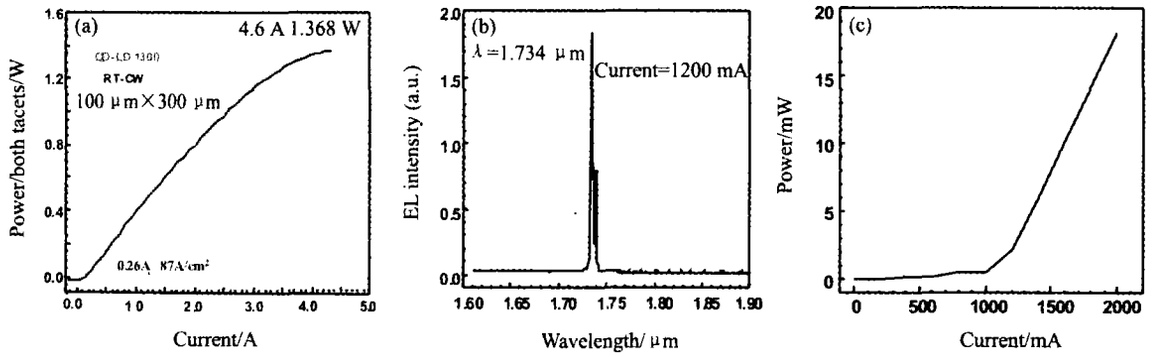

Fig. 4. (a) High performance 1.3 μm QD laser (RTCW0.6W is more than 6000 h), (b) and (c) are the lasing spectrum and I-V curve from a InP-based long wavelength QWR laser.

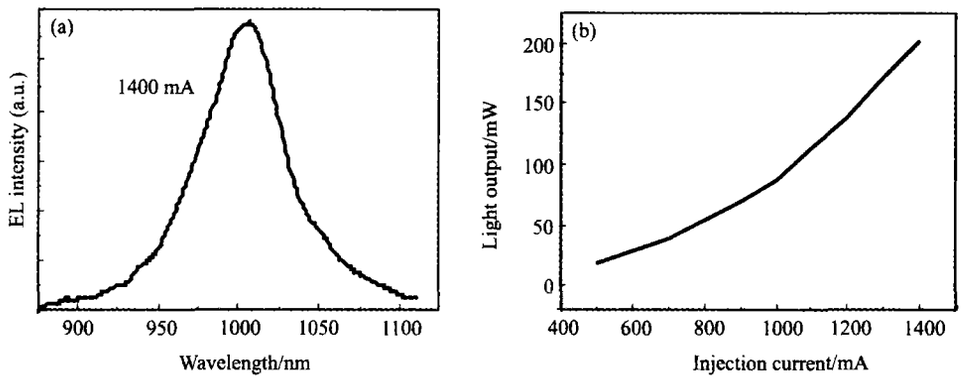

Fig. 5. The characteristics of quantum dot-SLD: (a) the spectral bandwidth 60 nm at RT, (b) CW output power 200 mW.

Typical double crystal X-ray diffraction (DXRD) results for QCL wafers are shown in Fig. 6. The appearance of numerous sharp and narrow satellite peaks indicates the excellent interface quality of the crystals. For both wafers, the zero-order superlattice X-ray diffraction peak shows a nearly perfect lattice match to the InP substrate, which indicates that the active region layers, based on $In_{1-x}Ga_xAs/In_{1-y}Al_yAs$, have been properly strain-balanced to give a net zero strain. The simulated results fitted pretty well with the experimental results. The simulated curves and experimental curves are nearly identical, indicating excellent uniformity and accurate control over the layer thicknesses, material compositions, and interface smoothness across the entire 30-period layer sequences. Double-channel ridge waveguide lasers of various cavity lengths were fabricated by photolithography and wet chemical etching. The lasers were bonded epilayer-side up on copper submounts with In solder and wire bonded. The spectral characteristics of the devices were measured using a Fourier transform infrared spectrometer. Optical power was measured from a single laser facet using a calibrated thermopile detector in ambient condition. The detector was placed directly in front of the laser facet and optical

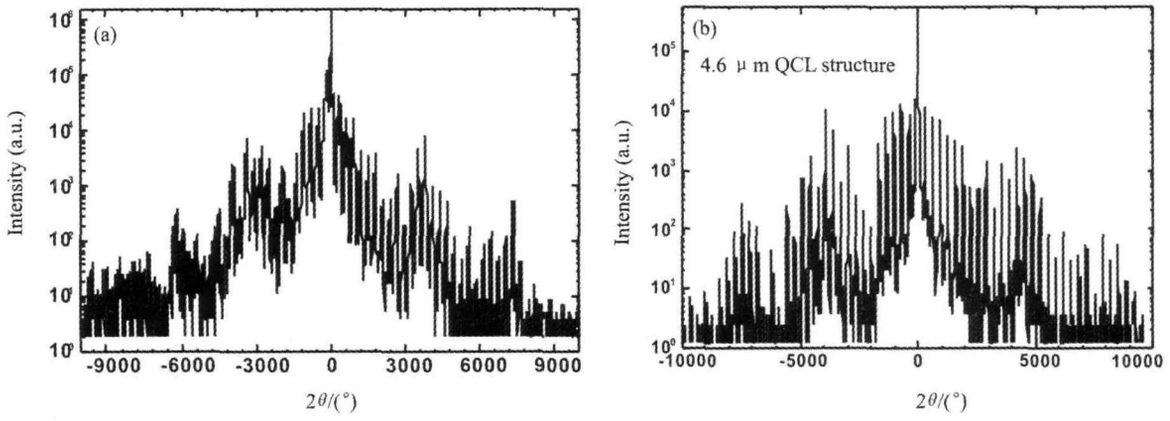

Fig. 6. DXRD results of QCL wafers for $\lambda \sim 7.4$ μm (a) and $\lambda \sim 4.6$ μm (b).

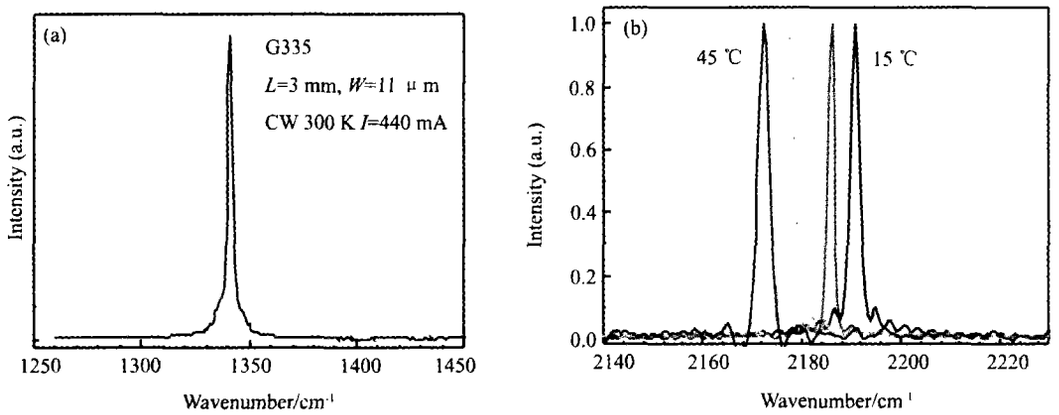

Fig. 7. RT CW lasing spectra of QCLs: (a) $\lambda \sim 7.4$ μm, (b) $\lambda \sim 4.6$ μm.

output power was measured without any correction.

Fig. 7 shows the emission spectra from 2 mm long and 12 μm wide devices at room temperature operated in CW mode. The laser characteristics reported here represent high performance of solid source MBE grown QCLs.

Acknowledgements

This work was supported by the State Key Development Program for Basics Research of China (Contract number: 2006CB6049), the National High Technology R&D program of China (Contract number: 2007AA03Z446), and the Key Program of National Natural Science Foundation of China (Contract number: 60736031).

References

[1] Z. C. Zhang, Y. H. Chen, Z. G. Wang, et al., *Semicond. Sci. Technol.*, 2003, **18**: 955.
[2] Z. Y. Zhang, Z. Wang, et al., *IEEE Photon. Technol. Lett.*, 2004, **16**: 27.
[3] F. Liu, Z. Wang, et al., *Semicond. Sci. Technol.*, 2000, **15**: L44.
[4] N. Liu, P. Jin, and Z. G. Wang, *Electronics Letters*, 2005, **41**(25): 1400.
[5] Yu Guo, F. Q. Liu, Z. Wang, et al., *Semicond. Sci. Technol.*, 2005, **20**(8): 844.
[6] Y. H. Chen, Z. Wang, et al., *Appl. Phys. Lett.*, 2006, **88**: 071903.
[7] Y. H. Chen, Z. Wang, et al., *Appl. Phys. Lett*., 2006, **88**: 071903.
[8] X. R. Yang, B. Xu, and Z. G. Wang, *Nanotech*, 2007, **18**(21): 215302.
[9] C. Zhao, Y. H. Chen, B. Xu, P. Jin, and Z. G. Wang, *Appl. Phys. Lett.*, 2007, **91**(3): 033112.